Nanoparticle Formation in Giant Vesicles: Synthesis in Biomimetic Compartments**

*Peng Yang, Reinhard Lipowsky, and Rumiana Dimova**

The formation of inorganic nanomaterials such as CdS, ZnS, and gold and silver nanoparticles was recently observed in microorganisms.[1] The underlying processes are still not well understood at the molecular scale. It has been proposed that enzymes or peptides may take part in the nucleation and reaction control.[2–4] It seems highly desirable to perform similar reactions in artificial systems as a first step towards biomimetic fabrication. Here, we introduce two novel protocols for nanoparticle synthesis in such artificial systems provided by giant vesicles. These membrane compartments have two main advantages. First, individual compartments can be manipulated by electric fields, micropipettes, or optical tweezers. Second, the particle formation process can be directly monitored using different microscopy techniques. Our protocols are based on the controlled fusion of such vesicles and on their adhesion via nanotubes. When these two protocols are applied to the synthesis of CdS nanoparticles, the particle size can be tuned to be 4 or 50 nm, which is in the range of quantum dot sizes. Our results show that controlled changes in the structure and topology of membrane compartments can be used to synthesize nanoparticles even in the absence of inorganic binding peptides.

Cells and microorganisms have been reported to have the amazing ability to synthesize inorganic nanoparticles.[1] The tentative interpretation of this observation is related to the involvement of specific molecules[2,3] such as inorganic-binding peptides,[3,4] which are also developed commercially to control nanoparticle synthesis in artificial cell-free reaction systems. In contrast to biochemistry-based cell-assisted synthesis, our present study aims at identifying mechanisms of nanomaterial synthesis in confined compartments provided by model biomembranes.

[*] Dr. R. Dimova, Dr. P. Yang,[+] Prof. R. Lipowsky
Department of Theory and Bio-Systems
Max Planck Institute of Colloids and Interfaces
Science Park Golm, 14424 Potsdam (Germany)
E-mail: rumiana.dimova@mpikg.mpg.de

[+] Current address: Department of Biomedical Engineering
Duke University
Durham, NC 27705, USA

[**] We would like to thank R. Knorr for his help with the confocal microscope. We acknowledge him and K. Tauer for critically reading the text.

Supporting Information is available on the WWW under http://www.small-journal.com or from the author.

DOI: 10.1002/smll.200900560

Giant unilamellar vesicles (GUVs), having dimensions in the cell-size scale (5–50 μm), provide a suitable system,[5] mimicking the confinement in cells or in the extracellular space. Their lipid membrane is impermeable to ions and macromolecules, while water can freely permeate through the membrane to assure osmotic balance. Thus, GUVs can be used as tiny compartments closed for reacting species. In this study, we take advantage of the small size of these compartments having volumes in the picoliter range to perform chemical synthesis. As an example, we considered the simple reaction $Na_2S + CdCl_2 \leftrightarrow CdS + 2NaCl$. When this reaction occurs in bulk, even at weak millimolar concentrations, irregular CdS sediments are formed because of the low solubility product constant of CdS ($K_{sp} = 10^{-27}\,M^2$ at 25 °C) and the significant source of ions in the solution. In the confined space of a giant vesicle, the source is quickly exhausted and smaller particles can be formed. We consider the following estimate: mixing 1 mM solutions of Na_2S and CdS in a vesicle with radius 10 μm can give yield to a CdS crystal not larger than $270 \times 270 \times 270\,nm^3$ if all ions take part in building it (here we assumed that the distance between the participating Cd atoms corresponds to an approximately 2 Å lattice spacing). In the event of mixing these two solutions, however, not one but many smaller particles may be nucleated and formed. The strategy of our experiments was to prepare vesicles containing either $CdCl_2$ or Na_2S and trigger the reaction either by vesicle fusion or by slow exchange and gradual mixing of the encapsulated solutions.

Up to now, nanoparticles have only been synthesized in lipid vesicles in the size range 30–80 nm (see, for example, References [6,7]), where the particle size would usually be determined by the vesicle volume. The vesicles were employed mainly to provide an initially closed container for the reaction. The attention was addressed towards the final reaction product, but no care was taken for preserving the membrane state and integrity during and after reaction completion. In contrast to nanometer-sized vesicles, using giant vesicles as microreactors allows for direct microscopy observation of the state of the membrane. Thus, this is the first time to induce, control, and directly observe particle formation in an artificial cell system whereby the membrane container remains intact. In addition, our study extends confined vesicular reactions to micrometer-scale cell-size reactors for the synthesis of nanomaterials. Finally, differently from the experimental conditions used previously for the synthesis of nanoparticles, here we employ processes mimicking intracellular mixing or membrane fusion, which naturally occur in cells.

The vesicles were prepared from the conventional lipid lecithin (egg phosphatidylcholine). To be able to distinguish them according to their content, two fluorescent lipids with different emission wavelengths were used in the preparation: one for vesicles containing Na_2S and another for vesicles loaded with $CdCl_2$. For simplicity, below we will refer to the two reactants as A and B. For the above mentioned reaction, A and B are simply Na_2S and $CdCl_2$, but the principles of our protocols apply to arbitrary chemicals as long as they can be encapsulated in GUVs. The latter is achieved by forming the vesicles in the presence of A or B, which is a process of swelling of lipid bilayers under the influence of weak alternating electric (AC) field (see the Supporting Information for details on the vesicle electroformation method in the presence of Na_2S and $CdCl_2$). The growing media contains A or B and is thus encapsulated in the vesicles. After having prepared the vesicles, we proceed with the two protocols for nanoparticle formation: fusion and slow content exchange.

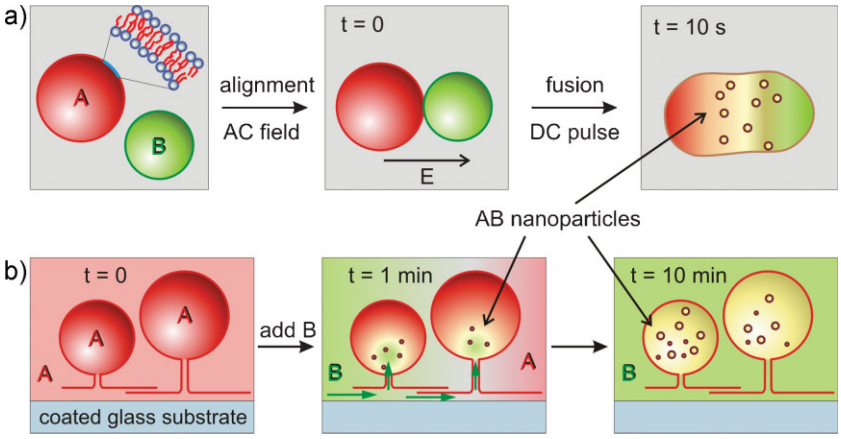

Figure 1. Two specifically designed protocols for performing inorganic nanomaterial synthesis in GUVs. a) Electrofusion-based method: vesicles containing reactant A and B are mixed (in A- and B-free environment) and subjected to an AC field to align them in the direction of the field and bring them close together. A DC pulse initiates the electrofusion of the two vesicles and the reaction between A and B proceeds to the formation of nanoparticles encapsulated in the fused vesicle. b) Slow content exchange method: Vesicles formed in the presence of A are still connected via nanotubes to the glass substrate of the electroformation chamber (see Supporting Information). The thickness of the nanotubes (tens of nm) and the size of the vesicles (tens of μm) are not in scale. Reactant B is slowly injected in the chamber. After diffusing through the nanotubes into the vesicle interior, B reacts with A to produce nanoparticles. The approximate timescales of the events are indicated in the pictures.

The fusion protocol is based on the application of strong electric pulses of short duration that induce electric breakdown of the lipid bilayers leading to formation of transient pores. The vesicles become permeable for a certain time (milliseconds).[8] When two such porated vesicles are in close contact, fusion occurs. The concept to utilize fusion of two GUVs to initiate content mixing reaction has been previously proposed,[9] but here for the first time we successfully use fusion of giant vesicles for the synthesis of nanomaterials.

According to our electrofusion protocol, after completing the electroformation process, the vesicles are detached from the substrate and placed in A- and B-free isotonic solution. Two vesicle populations are mixed, one loaded with A and labeled with one fluorescent dye (e.g., red), the other B-loaded and labeled differently (green). Application of the AC field aligns the vesicles in the direction of the field due to dielectric screening (similarly to pearl-chain formation in cell suspensions[10]). In order to monitor the nanoparticle formation process, we locate an A–B vesicle couple (red and green vesicles) and apply a direct current (DC) pulse strong and long enough to porate each of the vesicles (typically pulses of 0.5–2 kV cm^{-1} field strength and 150–300 μs duration suffice (see Supporting Information). The steps of this protocol are schematically illustrated in Figure 1a.

We expected that, upon particle formation, fluorescence is observed in the volume of the fused vesicle. Fluorescence in the wavelength range between 400 and 800 nm has been previously reported for CdS particles with diameters in the range 1–25 nm.[11] Indeed, direct observation of the fused vesicle with confocal microscopy indicated fluorescence in the interior of the fused vesicle (Figure 2). Because the confocal sections show only fluorescence from a thin slice of the vesicle, out-of-focus fluorescence, which might be emitted from the upper and lower part of the vesicle, is not detected. Intensity line profiles of the vesicles before and after fusion (Figure 2d–f), indicate the

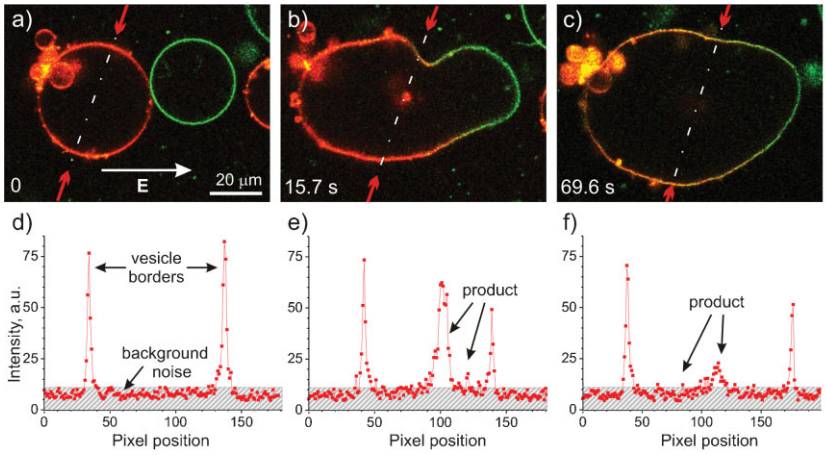

Figure 2. a–c) Confocal scans of vesicles loaded with 0.3 mM Na_2S (red) and 0.3 mM $CdCl_2$ (green) undergoing fusion. d–f) Intensity line profiles along the dash-dotted lines indicated by red arrows in (a–c), respectively. The direction of the field is indicated in (a). Before fusion (a and d), the vesicle interior shows only background noise similar to the external solution as indicated by the shaded zone in (d). After fusion (b, c, e, and f), fluorescence from the product is detected in the interior of the fused vesicle. The time after applying the pulse is indicated on the micrographs (for intermediate snapshots see Supporting Information and movie). The fluorescence signal was acquired in the ranges 565–765 nm (red channel) and 462–558 nm (green channel).

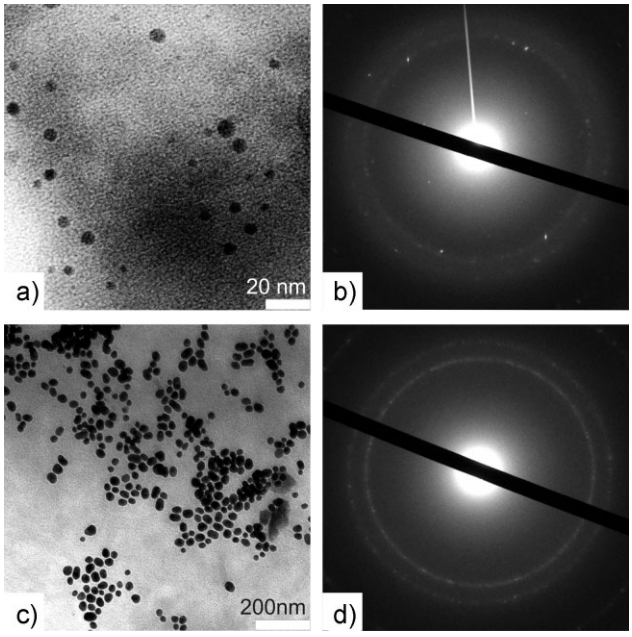

Figure 3. a) TEM image and b) SAED pattern from the product in the solutions after vesicle fusion. The salt concentration in the vesicles was 0.3 mM. Dispersed single-crystalline nanoparticles with diameter between 4 and 8 nm are detected. c) TEM image and d) SAED pattern from polycrystalline CdS nanopraticles in the chamber after the slow solution exchange. The salt concentration in the exchange solution and in the vesicles was 0.3 mM. The diameter of the nanoparticles is around 50 nm. The rings presumably represent averaged power diffraction.

presence of a product with fluorescence above the background noise signal. The signal is detectable for a few minutes before decaying completely (see Supporting Information). Presumably, capping of the nanoparticles with a shell (which, for example, can be achieved by successful fusion with vesicles loaded with the capping agent) may lead to stronger and long-term fluorescence as typical for commercial quantum dots.

The obtained product was also investigated using transmission electron microscopy (TEM) and selected area electron diffraction (SAED). Dispersed nanoparticles of diameters ranging between 4 and 8 nm were found (Figure 3a). The SAED pattern (Figure 3b) showed weak rings but also characteristic spotty patterns, indicating the single crystalline nature of the formed CdS nanoparticles. The rings presumably arise from the rupture of non-fused vesicles during TEM sample preparation. Thus, A and B could leak out from the non-fused vesicles and react via mixing. The rings were also observed for vesicle solutions not subjected to electrofusion, where only irregular sediments but no nanoparticles were found (see Supporting Information). In the fused samples, the vesicle fusion largely consumed the A and B source, so that the amount of irregular sediments was negligible.

The sizes of the formed nanoparticles correspond to the exciton Bohr radius of CdS (5–6 nm). Thus, the potential quantum effect from these quantum dot-sized CdS crystals was further examined for fluorescence from samples subjected to batch electrofusion (see Supporting Information). Significant fluorescence in the range 430–530 nm was detected, which can be attributed to the band gap emission and suggests high quality of the nanocrystals.[7,12]

The mixing of reactants during vesicle electrofusion occurs at very high speed because the opening of the fusion neck connecting the two fusing vesicles is rather fast with rates on the order of 5 cm s^{-1}.[13] Thus, within a few milliseconds the fusion creates a large interface with a cross section of the vesicle size where the two reactants are well mixed and the particles formed. Fast mixing of reactive precursors has been reported as an essential condition to produce CdS nanoparticles in microfluidic channels.[14] We emphasize that the protocol described above and the rate of mixing in fusing vesicles is independent of the way fusion is induced,[13] that is, whether it would be triggered by a ligand–receptor type of interaction (as in cells where fusion proteins are involved[15] or in biomimetic systems[13,16]) or by electrofusion as applied in this work. Thus, our experiments suggest that in vivo, the fusion of small vesicles with the cell membranes might infer a possible mechanism for the cell-based synthesis of nanoparticles. The necessary condition according to such a scenario is that the vesicles are loaded with reactant A, while the local concentration of B at the cell is suitably matched. Our results demonstrate that low concentrations in the submillimolar range are sufficient to produce CdS nanoparticles.

The second protocol we applied, the slow content exchange protocol, mimics the incubation stages during the process of cellular inorganic nanoparticle synthesis.[1] This protocol is not based on external perturbations such as a strong electric pulse, but on the fact that, during formation, the majority of vesicles remains connected to the substrate via lipid nanotubes or tethers (see the first cartoon in Figure 1b). The latter have a typical diameter in the 50–100 nm range and are optically detectable with fluorescence (see Supporting Information). We prepared vesicles containing reactant A and slowly exchanged the external medium with solution containing reactant B (Figure 1b and see Supporting Information). During this slow exchange, which takes 10–15 min, the vesicles remain connected to the substrate and reactant B diffuses into the vesicle interior through the connecting tethers leading to particle formation (note that the membrane of the vesicle is impermeable to ions and no direct leakage from the vesicle body occurs). TEM images as in Figure 3c showed bigger nanoparticles with diameters around 50 nm, that is, beyond the range of typical quantum dot sizes, which are smaller than or comparable to 10 nm. The larger particle size may imply a smaller number of crystal nuclei. The particles were polycrystalline as demonstrated by the two diffraction rings in the corresponding SAED pattern[17] (Figure 3d). They also showed enhanced fluorescence (see Supporting Information). For the slow content exchange protocol, our setup did not allow us to perform confocal microscopy scans and image analysis as in Figure 2 because of the large thickness of the substrate. Thus we were not able to identify whether the nanoparticles were formed in the vesicle volume or in the nanotubes connecting them with the substrate. The solution flown out of the chamber, which consisted of a mixture of the introduced B and the reagent A from the vesicle exterior, contained irregular sediment with poor polycrystalline structure (see Supporting Information).

To summarize, this work reports two successful biomimetic approaches for nanoparticle synthesis in GUVs, which represent membrane-bound compartments. Our results suggest that the possible mechanism of cell-based nanoparticle synthesis, whether intra- or extracellular, may not necessarily be only peptide- or protein-driven or regulated. Simple chemical mixing of subpicoliter volumes due to fusion of carrier vesicles with cell membranes or slow influx in the intracellular space may be the possible pathway of these syntheses. Here, we demonstrated the feasibility of nanoparticle formation in giant vesicles. The sizes of CdS nanoproducts synthesized could be tuned to be 4 or 50 nm in diameter using two different protocols. Improving the yield for the electrofusion protocol is a matter of applying batch electrofusion in optimized electrofusion chambers (see Supporting Information).

In peptide-assisted synthesis, the involvement of the peptides could be related to lowering of the critical nucleation size and controlling the crystal morphology. In comparison, nanoparticle synthesis in vesicles is presumably surface nucleated, while the particle size and number is determined by the finite volume of the membrane compartment. Surface nucleation can be modulated by the membrane composition (either lipid or polymer as in liposomes or polymersomes, respectively). Localization of the particle nucleation to a specific site at the membrane should be feasible using multicomponent lipid vesicles with surface domains.[5] Furthermore, phase separation and wetting transitions of aqueous solutions in giant vesicles as reported recently[18] could also be used in order to restrict the particle formation process to particular segments of the membrane surface or to interrupt it by dewetting. Based on the potential of GUV for biomimetic nanomaterials preparation demonstrated here, we expect that novel approaches for performing various inorganic and/or organic synthesis using GUVs as microreactors can be developed, which is currently an insufficiently explored field.

Experimental Section

Vesicle preparation: The precondition for successful nanoparticle synthesis is the preparation of GUVs containing $CdCl_2$ and Na_2S. We employed the method of electroformation[5] (see Supporting Information), which, to our knowledge, has not been previously used to form vesicles in the presence of $CdCl_2$ and Na_2S. We found that, when using the conventional electroformation method, vesicle quality and yield in the presence of $CdCl_2$ at concentrations higher than about 0.3 mM drastically decreased, while the concentration limit was higher and about 3 mM for Na_2S. Similarly to other cations like Ca^{2+} and Mg^{2+},[19] possible binding of Cd^{2+} to the lipid headgroups may modify the bilayer properties and impede bilayer swelling and vesicle formation. This assumption is consistent with the observed increase of the membrane bending stiffness in the presence of salts.[20]

Electrofusion protocol: Previously, we have used this approach to prepare vesicles of composite membranes starting from vesicle couples with the same volume content but different lipid composition.[5] Here, the vesicles differ in their encapsulated solutions. The vesicles are detached from the substrate of the electroformation chamber and significantly diluted in A- and B-free isotonic solution, for example, glucose. For $CdCl_2$-loaded vesicles, the solution was in addition left in contact with ion-exchange resin (Amberlite IR-120, H^+ form, Sigma-Aldrich, Germany) to remove all Cd^{2+} from the vesicle exterior. Populations of A- and B-loaded vesicles are mixed and the solution is placed in a chamber with two cylindrical parallel electrodes. The AC field (3V, 2 MHz) is applied for 90 s. Then, an A- and B-loaded vesicle couple is selected for confocal microscopy observation and subjected to a DC pulse (typically of field strength 0.5–2 kV cm^{-1} and duration 150–300 μs). The process is observed with a confocal microscope (Leica TCS SP5) with a 63× water immersion objective at room temperature and excitation wavelengths of 488 and 561 nm. The scanning confocal acquisition speed is relatively slow compared to diffusion of nanoparticles, which is why the fluorescence in the fusion zone as shown in Figure 2b appears diffuse (typically the acquisition of an image of 512×512 pixels^2 takes about 1.3 s).

Electrofusion between A- and B-loaded vesicles was found to proceed smoothly at lower reagent concentrations (≤0.3 mM). Tests on similarly loaded A–A and B–B couples at higher A and B concentrations showed that the inhibition of the electrofusion state might arise from specific effects of binding of Cd^{2+} presumably influencing the membrane rigidity (similar to effects of calcium as discussed in the section on vesicle preparation) and inhibiting the opening of the fusion neck (see Supporting Information).

Nanoparticle characterization: The products from vesicle electrofusion and slow content mixing were characterized using an Omega 912 TEM (Carl Zeiss, Oberkochen, Germany) with 100 kV accelerating voltage. Fluorescence spectra were measured with luminescence spectrometer LS50B (Perkin Elmer, Beaconsfield, England) with excitation at 400 nm.

Keywords:

biomimetic synthesis · membranes · nanostructures · quantum dots · vesicles

[1] a) D. Bhattacharya, R. K. Gupta, *Crit. Rev. Biotechnol.* **2005**, *25*, 199; b) D. Mandal, M. E. Bolander, D. Mukhopadhyay, G. Sarkar, P. Mukherjee, *Appl. Microbiol. Biotechnol.* **2006**, *69*, 485; c) C. Sanchez, H. Arribart, M. Madeleine, G. Guille, *Nat. Mater.* **2005**, *4*, 277; d) R. Y. Sweeney, C. B. Mao, X. X. Gao, J. L. Burt, A. M. Belcher, G. Georgiou, B. L. Iverson, *Chem. Biol.* **2004**, *11*, 1553.

[2] a) P. Mukherjee, A. Ahmad, D. Mandal, S. Senapati, S. R. Sainkar, M. I. Khan, R. Ramani, R. Parischa, P. V. Ajayakumar, M. Alam, M. Sastry, R. Kumar, *Angew. Chem.* **2001**, *113*, 3697; *Angew. Chem. Int. Ed.* **2001**, *40*, 3585; b) A. Ahmad, P. Mukherjee, D. Mandal, S. Senapati, M. I. Khan, R. Kumar, M. Sastry, *J. Am. Chem. Soc.* **2002**, *124*, 12108; c) C. T. Dameron, R. N. Reese, R. K. Mehra, A. R. Kortan, P. J. Carroll, M. L. Steigerwald, L. E. Brus, D. R. Winge, *Nature* **1989**, *338*, 596; d) M. Umetsu, M. Mizuta, K. Tsumoto, S. Ohara, S. Takami, H. Watanabe, I. Kumagai, T. Adschiri, *Adv. Mater.* **2005**, *17*, 2571.

[3] N. Kröger, M. B. Dickerson, G. Ahmad, Y. Cai, M. S. Haluska, K. H. Sandhage, N. Poulsen, V. C. Sheppard, *Angew. Chem.* **2006**, *118*, 7397; *Angew. Chem. Int. Ed.* **2006**, *45*, 7239.

[4] R. R. Naik, S. J. Stringer, G. Agarwal, S. E. Jones, M. O. Stone, *Nat. Mater.* **2002**, *1*, 169.

[5] R. Dimova, S. Aranda, N. Bezlyepkina, V. Nikolov, K. A. Riske, R. Lipowsky, *J. Phys.: Condens. Matter* **2006**, *18*, S1151.

[6] a) S. Mann, J. P. Hannington, R. J. P. Williams, *Nature* **1986**, *324*, 565; b) S. Bhandarkar, A. Bose, *J. Colloid Interface Sci.* **1990**, *139*, 541.
[7] a) M. I. Khramov, V. N. Parmon, *J. Photochem. Photobiol. A* **1993**, *71*, 279; b) B. A. Korgel, H. G. Monbouquette, *Langmuir* **2000**, *16*, 3588.
[8] K. A. Riske, R. Dimova, *Biophys. J.* **2005**, *88*, 1143.
[9] a) D. T. Chiu, C. F. Wilson, F. Ryttsen, A. Stromberg, C. Farre, A. Karlsson, S. Nordholm, A. Gaggar, B. P. Modi, A. Moscho, R. A. Garza-Lopez, O. Orwar, R. N. Zare, *Science* **1999**, *283*, 1892; b) S. Kulin, R. Kishore, K. Helmerson, L. Locascio, *Langmuir* **2003**, *19*, 8206.
[10] U. Zimmermann, *Rev. Physiol. Biochem. Pharmacol.* **1986**, *105*, 176.
[11] H. Weller, *Angew. Chem.* **1993**, *105*, 43; *Angew. Chem. Int. Ed.* **1993**, *32*, 41.
[12] J. A. Gratt, R. E. Cohen, *J. Appl. Polym. Sci.* **2003**, *88*, 177.
[13] C. K. Haluska, K. A. Riske, V. Marchi-Artzner, J. M. Lehn, R. Lipowsky, R. Dimova, *Proc. Natl. Acad. Sci. USA* **2006**, *103*, 15841.
[14] I. Shestopalov, J. D. Tice, R. F. Ismagilov, *Lab Chip* **2004**, *4*, 316.
[15] R. Jahn, T. Lang, T. C. Südhof, *Cell* **2003**, *112*, 519.
[16] A. Richard, V. Marchi-Artzner, M. N. Lalloz, M. J. Brienne, F. Artzner, T. Gulik-Krzywicki, M. A. Guedeau-Boudeville, J. M. Lehn, *Proc. Natl. Acad. Sci. USA* **2004**, *101*, 15279.
[17] S. Gorer, J. A. Ganske, J. C. Hemminger, R. M. Penner, *J. Am. Chem. Soc.* **1998**, *120*, 9584.
[18] Y. Li, R. Lipowsky, R. Dimova, *J. Am. Chem. Soc.* **2008**, *130*, 12252.
[19] a) R. A. Bockmann, H. Grubmuller, *Angew. Chem.* **2004**, *116*, 1039; *Angew. Chem. Int. Ed.* **2004**, *43*, 1021; b) C. Sinn, M. Antonietti, R. Dimova, *Colloids Surf. A* **2006**, *283*, 410.
[20] G. Pabst, A. Hodzic, J. Strancar, S. Danner, M. Rappolt, P. Laggner, *Biophys. J.* **2007**, *93*, 2688.

Received: April 1, 2009
Published online: June 8, 2009

Submitted to small

Supporting Information on "Nanoparticle Formation in Giant Vesicles: Synthesis in Biomimetic Compartments"

Peng Yang[#], Reinhard Lipowsky, Rumiana Dimova[*]

Max Planck Institute of Colloids and Interfaces, Science Park Golm, 14424 Potsdam, Germany
[#] Present address: Department of Biomedical Engineering, Duke University, Durham, NC 27705
* Address correspondence to: rumiana.dimova@mpikg.mpg.de

Vesicle preparation and observation. Cadmium chloride ($CdCl_2$) and anhydrous sodium sulfide (Na_2S) were purchased from Sigma (St. Louis, MO) and used as received. Only freshly prepared salt solutions in ultrapure water were used in every experiment. Giant unilamellar vesicles (GUV) were prepared from egg yolk L-α- phosphatidylcholine (Egg-PC) (Sigma) using a procedure described in detail in [1]. Briefly, Egg-PC was dissolved in chloroform to form 2 mg/ml lipid solution. For observation of the vesicles with fluorescence microscopy the following dyes were used: 1,1'-dioctadecyl-3,3,3',3'-tetramethylindocarbocyanine perchlorate ($DiIC_{18}$) from Molecular Probes (Leiden, The Netherlands; excitation wavelength at 551 nm and emission wavelength at 569 nm) was added to the lipid solution at concentration 0.1 mol %, and perylene from Sigma-Aldrich (Steinheim, Germany; with excitation wavelength at 440 nm and emission wavelength at 450 nm) was added at concentration 0.4 mol %. Typically, for the Na_2S-loaded vesicles we used $DiIC_{18}$ as fluorescence marker and for the $CdCl_2$-loaded vesicles we used perylene. A small drop (~ 50 µl) of lipid solution was placed onto a glass slide coated with indium tin oxide (ITO) and spread evenly on the surface. Two such coated ITO glasses are placed in a vacuum desiccator at room temperature for at least 2 h to evaporate the organic solvent. For the vesicles grown in the presence of $CdCl_2$, we found out that drying at higher temperature (60°C) yields more and bigger vesicles. A closed chamber was assembled from the two ITO glasses (the sides with conductive coating were facing each other) and a 1 mm thick rectangular Teflon spacer with two holes as solution inlet and outlet. The $CdCl_2$- and Na_2S-loaded vesicles for the electrofusion protocol were typically grown in parallel. The growing solution ($CdCl_2$ or Na_2S in 100 mOsm sucrose) was introduced through the inlet to fill the respective chamber. The chambers were connected in parallel to an AC field function generator (Agilent 33220A 20 MHz function/arbitrary waveform generator) and an alternating voltage with amplitude of 0.7 V (peak-to-peak) and frequency of 10 Hz was applied for 4 h. The AC voltage was a key parameter for the formation of $CdCl_2$-loaded vesicles. In 0.03 mM $CdCl_2$ solution, GUVs were formed at low voltage (< 1.7 V). At higher voltages, the vesicles would start rupturing. However, for electroformation of Na_2S-loaded vesicles, even in 3 mM Na_2S solution, this effect was not observed. Presumably, $CdCl_2$ affects the membrane properties making the bilayers either more fragile or inducing additional tension (as previously observed with solutions containing calcium).[2]

For the protocol with slow solution exchange, the vesicles were used as formed in the chamber.

For the electrofusion protocol, the vesicles were detached from the ITO glass substrate by lowering the field frequency to 5 Hz and setting the voltage to 0.5 V for 20 min. Then, the vesicles were removed from the electroformation chamber, diluted up to 40 times with isotonic glucose solution, and transferred into an electrofusion chamber (Eppendorf, Germany). The latter consists of a Teflon frame with two cylindrical electrodes (500 µm in diameter) with a gap distance of 200 µm. The chamber was connected to a Multiporator (Eppendorf, Germany) to align the vesicles (AC field of 3 V, 2 MHz for 90 s applied a few times) and electrofuse them (DC pulses of field strength 0.5-2 kV/cm and 150-300 µs duration). The glucose-sucrose asymmetry creates a density difference

stabilizing the vesicles at the bottom of the chamber. The vesicles and the fusion process are observed by laser scanning confocal microscopy (Leica, TCS SP5, Germany) with excitation at 458 nm (Ar laser) for perylene and 561 nm (DPSS laser) for $DiIc_{18}$.

Details about the electrofusion protocol. The electrofusion between $CdCl_2$-loaded GUVs and Na_2S-loaded GUVs showed an interesting dependence on salt concentration. The electrofusion could only proceed smoothly at low salt concentration ($\leq$ 0.3 mM); see SI Movie. Higher salt concentration, for example 3 mM, would hinder electrofusion between two differently or equally loaded vesicles. A possible interpretation for the inability such $CdCl_2$-loaded GUV to fuse is that cadmium binding to the membranes could increase their rigidity and block the formation of transmembrane fusion pore.

For vesicles loaded with lower salt concentrations, fusion proceeds as described in the main text. A sequence of snapshots corresponding to Fig. 2 in the main text is given in Fig. S1. The SI Movie and Fig. S1 show the electrofusion between $CdCl_2$-loaded GUV and Na_2S-loaded GUV. Subsequent inspection of vesicles sections above and below the scanning plane showed no presence of membrane inclusions (free vesicles or membrane fractions) in the fusion zone. Therefore, the source of fluorescence is provided by the formed nanoparticles.

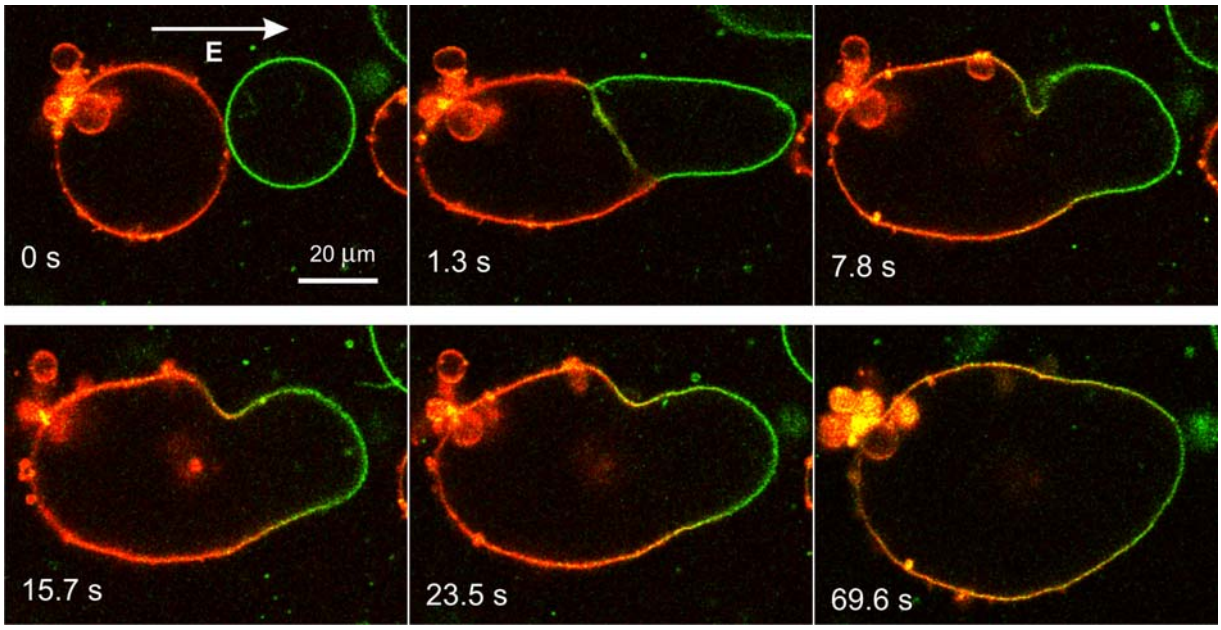

Figure S1 Confocal scans of vesicles loaded with 0.3 mM Na_2S (red) and 0.3 mM $CdCl_2$ (green) undergoing fusion after being subjected to an electric pulse (excitation wavelengths: 458 nm and 561 nm). The fluorescence signal has been acquired in the ranges 565-765 nm (red channel) and 462 - 558 nm (green channel). The field direction is indicated by the arrow in the first snapshot. The acquisition time is indicated on every image, where t = 0 s corresponds to the last snapshot before applying the pulse. Several seconds after fusion, a fluorescence signal is detected from the product in the vesicle interior (note that only fluorescence from objects located in the focal plane is visible in the images; particles out of focus are not detected). The signal, both from the membrane and from the vesicle interior, decays with time. The images shown in this figure represent six snapshots from the SI Movie.

Transmission electron microscopy (TEM) and selected area electron diffraction (SAED) on vesicle solutions subjected to electrofusion, demonstrated the presence of nanoparticles as shown in Fig. 3a,b in the main text (note that these samples were obtained from batch electrofusion, which provides higher yield; see next section). As a reference test, we also examined mixed vesicle

solutions before electrofusion. They showed the presence of irregular sediments similar to those reported in [3] as demonstrated by TEM; see Fig. S2a. The SAED pattern showed two widened diffraction rings (Fig. S2b) due to multiple overlapping from the following CdS crystalline lines: (100), (002), (101) for the inner diffraction ring and (110), (103), (112) for the outer ring.[4] This implies that the product was polycrystalline with poor crystalline orientation. Even though Cd^{2+} in the vesicle exterior were entirely removed before mixing the vesicle solutions, polycrystalline CdS in samples not subjected to electrofusion was detected because of the TEM sample preparation procedure. In particular, $CdCl_2$- and Na_2S-loaded vesicles tend to rupture when dried on the TEM grid and the released reagents react via mixing.

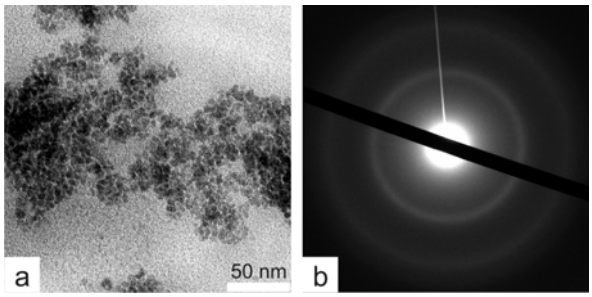

Figure S2 TEM image (a) and SAED pattern (b) from a solution of Na_2S- and $CdCl_2$-loaded vesicles not subjected to electrofusion. The reagent concentration in the vesicles was 0.3 mM. Only irregular sediments with pour crystalline structure are formed due to vesicle rupture upon deposition on the TEM grid and subsequent content mixing.

The potential quantum effect from the quantum dot-sized CdS crystals formed during the vesicle electrofusion (as shown in Fig. 3a,b in the main text) was examined for fluorescence and compared with the signal from solutions not subjected to electrofusion; see Fig. S3. Significant fluorescence in the range 430–530 nm was detected for the electrofusion sample, which can be attributed to the band gap emission and suggests high quality of the nanocrystals.[5-7] Moreover, the absence of emission at higher wavelengths (up to 700 nm) associated with deep trapped states due to surface or core defects, indicates the high quality of the nanocrystals. Note that for these measurements, the excitation wavelength was 400 nm while the confocal scans in Fig. S1 were obtained by excitation with a laser at 458 nm.

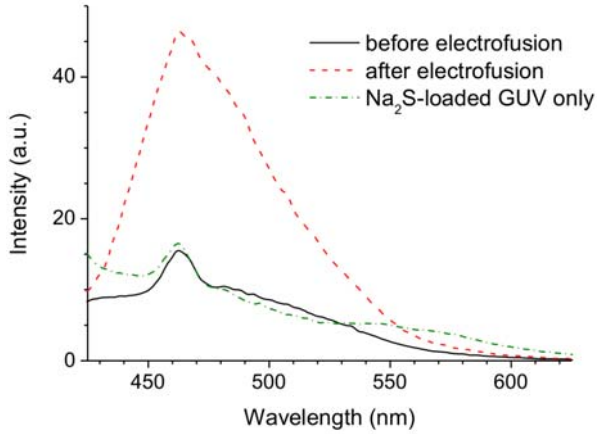

Figure S3 Fluorescent spectra of the samples before (solid black curve) and after electrofusion (dashed red curve). As a control test, the fluorescence signal from Na_2S-loaded GUV solution is also plotted (dash-dotted green curve). The excitation wavelength is 400 nm. The resulting fluorescent emission at around 460 nm is strongly enhanced after electrofusion.

Batch electrofusion. The example shown in Fig. 2 of the main text represents the fusion of one vesicle couple selected under the microscope. To perform the TEM, SAED and fluorescence measurements, one needs a sample that contains a large fraction of fused vesicles. In order to increase the yield from the electrofusion protocol we applied batch electrofusion where a larger fraction of vesicles fuse. This was achieved by increasing the volume of concentrated vesicle solution located between the two electrodes. For this purpose, we used a helix fusion chamber (Eppendorf, Germany), which consists of two coil (helix) electrodes with gap distance 250 μm and a total volume of 250 μl. This volume is more than 20 times larger than the one between the two straight cylindrical electrodes as used for the microscopy experiments, and thus allowing higher yield. Furthermore, for the microscopy observation the vesicles were additionally diluted to ensure no interference of neighboring vesicles in the image.

A prerequisite for the successful batch electrofusion was to remove the free Cd^{2+} ions from the exterior of the $CdCl_2$-loaded vesicles before mixing them with the Na_2S-loaded ones. The $CdCl_2$-loaded vesicles were placed in contact with ion-exchange resin (Amberlite IR-120, H^+ form, Sigma-Aldrich, Germany). The resin was thoroughly washed beforehand to remove small molecular impurities (3 times in deionized water), then activated according to the instructions of the manufacturer (acid wash with 2N HCl, at least 3 times), and rinsed at least 10 times with deionized water to pH > 5. The vesicles electroformed in $CdCl_2$ solution were then added to the resin at optimized condition (200 mg resin for 2 ml $CdCl_2$-loaded GUV solution under very slow stirring for 1 hr). After the removal of the Cd^{2+} ions outside the vesicles, 1 ml solution of $CdCl_2$-loaded GUV was mixed with 1 ml solution of Na_2S-loaded GUV. Half of the mixture was used as a reference sample, while the rest was subjected to electrofusion in the helix fusion chamber in 4 portions of 250 μl each. The AC field (9 V, 2 MHz) was applied to each portion for about 15 min, followed by one pulse of 300 V and 150 μs duration. The 4 aliquots were then collected and subjected to further analysis using TEM and fluorescence spectroscopy.

Slow content exchange protocol. The vesicles were electroformed in Na_2S solution and left in the chamber. The preparation process leads to the formation of vesicles, which are connected to the substrate via lipid nanotubes (tethers). To visualize the tethers (see Fig. S4) we prepared the vesicles on cylindrical platinum electrodes where side view observation of the growing vesicles is possible with *xy*-scans (contrary to the case when the vesicles are grown on ITO plates where *z*-scans are necessary to observe the tethers; the latter was not possible due to the large thickness of the ITO substrates). Typically, these tethers can be broken (releasing the vesicles) if the frequency of the applied AC field is reduced to about 5 Hz for ten minutes. For the protocol used here, we did not apply this latter procedure. Instead, the electroformation chamber that contained the vesicles tether-bound to the substrate was connected to a polyvalent syringe pump (Lambda Vit-fit, the Czech Republic), which slowly exchanged the solution without detaching the vesicles from the substrate. The injection speed influences the shape and transformation of the attached GUV.[8-9] The optimal injection speed was about 1 ml/min. To ensure complete replacement of the external solution, the total injection volume was at least four times the volume of the chamber. The solution flown out of the chamber was collected. Then, the frequency of the applied AC field was lowered to 5 Hz for 20 min to detach the GUV from the ITO substrate and collected separately for inspecting the product formed within the vesicles.

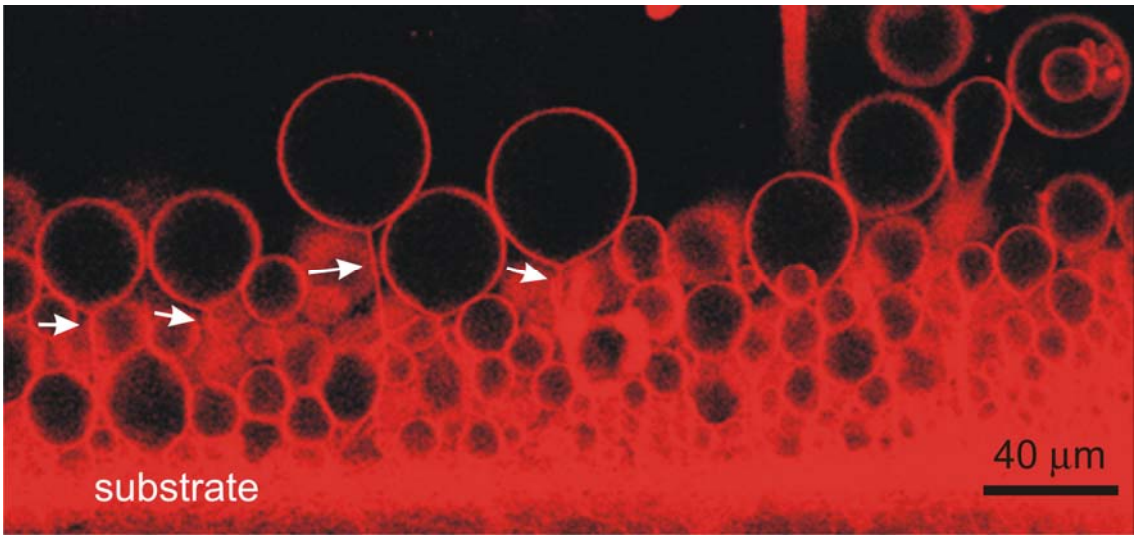

Figure S4 Confocal scan through a chamber with vesicles electroformed on cylindrical electrodes. At the end of the preparation procedure, the vesicles remain connected to the substrate (electrode) via nanotubes (indicated by arrows). Note that tethers, which are slightly behind or in front of this scanning plane, are not imaged.

The solution in the chamber and the one flown out before detaching the vesicles were examined using TEM and fluorescence spectroscopy. The chamber solution with the vesicles showed the presence of nanoparticles as demonstrated in Fig. 3c,d of the main text. The solution flown out of the chamber (a mixture of the introduced B and the reagent A from the vesicle exterior) contained only irregular sediments;[3] see Fig. S5.

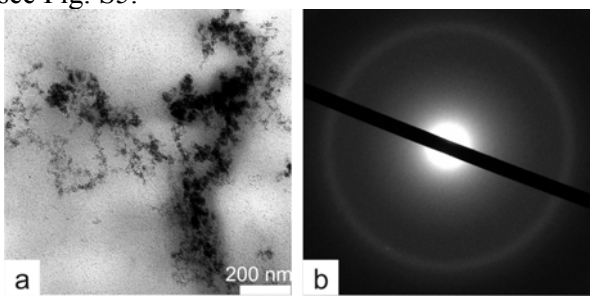

Figure S5 TEM image (a) and SAED pattern (b) from sediments with poor polycrystalline structure in the solution flown out of the chamber. The reagent concentration in the exchange solution and in the vesicles was 0.3 mM.

The fluorescence spectrum of the solution in the chamber with the vesicles after the content exchange, see Fig. S6, showed an enhanced signal around 460 and 570 nm, which can be associated with the band gap emission and surface or core defect trapped states. For comparison, the solution flown out of the chamber that contained $CdCl_2$ injected in the chamber and Na_2S present in the vesicle exterior showed a signal that is similar to the one obtained from direct mixing of the two reagents.

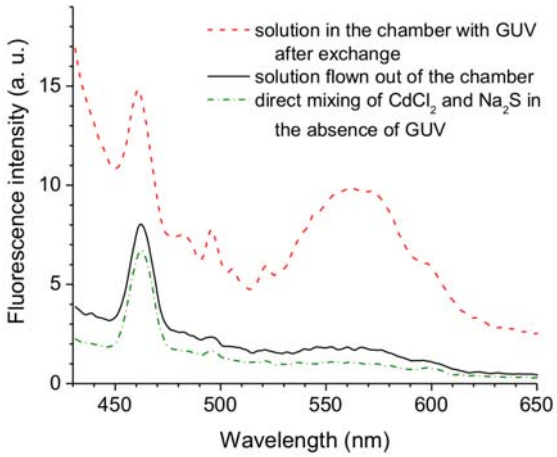

Figure S6 Fluorescent spectra of the sample containing the vesicles and the one flown out of the chamber. The solution in the chamber with GUV after the content exchange protocol (dashed red curve) has significant absorption in the range 460-600 nm due to the formed nanoparticles. This signal is not observed from the solution flown out of the chamber (solid black curve). For comparison, the fluorescence spectra from direct mixing of $CdCl_2$ and Na_2S solutions with the same concentration (0.3 mM) is also plotted (dash-dotted green curve).

Supplementary movie. The SI Movie shows the fusion between $NaCl_2$-loaded and $CdCl_2$-loaded vesicles, snapshots of which are presented in Fig. S1. The event is displayed about 10 times faster than in reality (the real time duration of the movie is about 90 seconds).

References

[1]. K. A. Riske, R. Dimova, *Biophys. J.* **2005**, *88*, 1143.
[2]. C. Sinn, M. Antonietti, R. Dimova, *Colloid Surf. A-Physicochem. Eng. Asp.* **2006**, *283*, 410.
[3]. R. Radvan, N. Popovici, R. Savastru, C. Ghica, F. Sava, M. Popescu, *J. Optoelectron. Adv. Mater.* **2001**, *3*, 897.
[4]. H. L. Li, Y. C. Zhu, S. G. Chen, O. Palchik, J. P. Xiong, Y. Koltypin, Y. Gofer, A. Gedanken, *J. Solid State Chem.* **2003**, *172*, 102.
[5]. B. A. Korgel, H. G. Monbouquette, *Langmuir* **2000**, *16*, 3588.
[6]. M. I. Khramov, V. N. Parmon, *J. Photochem. Photobiol. A-Chem.* **1993**, *71*, 279.
[7]. J. A. Gratt, R. E. Cohen, *J. Appl. Polym. Sci.* **2003**, *88*, 177.
[8]. D. J. Estes, M. Mayer, *Biochim. Biophys. Acta.* **2005**, *1712*, 152.
[9]. D. J. Estes, S. R. Lopez, A. O. Fuller, M. Mayer, *Biophys. J.* **2006**, *91*, 233.